Characterization of scoria rock from Arabian lava fields as natural pozzolan for use in concrete

Galal Fares, Abdulrahman Alhozaimy, Abdulaziz Al-Negheimish & Omer Abdalla Alawad

Published online: 12 Sep 2019.

Submit your article to this journal

View related articles

View Crossmark data

Taylor & Francis
Taylor & Francis Group

Check for updates

Characterization of scoria rock from Arabian lava fields as natural pozzolan for use in concrete

Galal Fares[a] (iD), Abdulrahman Alhozaimy[a], Abdulaziz Al-Negheimish[a] and Omer Abdalla Alawad[b]

[a]Center of Excellence for Concrete Research and Testing, Department of Civil Engineering, College of Engineering, King Saud University, Riyadh, Saudi Arabia; [b]Department of Civil and Environmental Engineering, College of Engineering, Majmaah University, Al Majmaah, Saudi Arabia

ABSTRACT

The feasibility studies of using alternative cementitious materials (ACMs) in concrete construction are conducted using various characterization tests. Different samples of scoria rocks (SR) were procured from different regions of the Arabian Shield and investigated for use as ACMs. Various methods and characterization techniques were conducted. Characterization results revealed that the pozzolanic activity of SR in mortar does not correlate well with the sum of the main elemental oxides $(SiO_2+Al_2O_3+Fe_2O_3)$, as per the requirement of ASTM C618. Concrete mixtures containing 30% SR per cement weight were prepared and tested at 28 and 90 days to evaluate the performance of SR for construction applications. Furthermore, the mortar and concrete mixtures containing SR have shown a slow rate of pozzolanic activity at early ages. However, the development in compressive strength was enhanced at later ages dependent on the mineralogical compositions of SR. It is concluded that the improvement in strength could be corroborated based on the formation of tobermorite-like structures, as confirmed using XRD and thermal analyses. These structures result from the reaction of minerals of amorphous sodium aluminosilicate phase (albite minerals) in SR with portlandite liberated during cement hydration. Conclusively, SR reacts as a pozzolan not as a filler.

1. Introduction

In many parts of the world, including Turkey, USA, Mexico, Papua New Guinea, and Arabian Peninsula, there are massive areas of Cenozoic volcanic rocks. These large areas are composed of lava flows and volcanic deposits identified as scoria rocks (SR) for the use as natural pozzolans (Al-Swaidani & Aliyan, 2015; Hossain, 2006; Moufti, Sabtan, El-Mahdy, & Shehata, 1999, 2000). Many researchers have investigated the use of natural pozzolans in paste, mortar, and concrete mixtures as a mineral additive or binder ready to be activated. For example, Shi and Day (1993) investigated the ancient method of activating natural pozzolans using lime incorporated with other inorganic sulfate and chloride salts as chemical activators. A maximum strength of 14 MPa at 90 days was reported. Others have investigated the use of natural pozzolans as an additive with cement in mortar and concrete for elevated strength and improved properties (Aldossari,

Fares, & Ghrefat, 2019; Celik et al., 2014; Colak, 2003; Khan & Alhozaimy, 2011; Fares, Alhozaimy, Alawad, & Al-Negheimish, 2017). In this context, Turanli, Uzal, and Bektas (2004) investigated the effect of elevated replacement levels of natural pozzolans on the mechanical properties of various blended cement pastes and mortars at 91 days. It is concluded that the improving effect of high volume of natural pozzolans on expansion due to sulfate resistance and alkali–silica activity was substantial. Similarly, Cavdar and Yetgin (2007) worked on the pozzolanic activities of six types of different tuff samples collected from two regions at the Northeast of Turkey. Mortar samples made of slaked lime and those types of natural pozzolans. These samples were then cast and tested for compressive and flexural strengths at 7 days according a relevant Turkish standard. The relationships between elemental oxides and mechanical properties were established. From these relationships, it is concluded that an increase in the proportion of SiO_2 in the pozzolan increases the pozzolanic activity. In the same way, Senhadji, Escadeillas, Khelafi, Mouli, and Benosman (2012) studied the use of natural pozzolans procured from a source in Northwestern of Algeria as mineral addition in the range of 0–25%. Different tests such as setting times, compressive strength, heat of hydration and XRD analyses of the hydration products were conducted to evaluate the pozzolanic activity of natural pozzolans. It is mentioned that the optimum dosage to obtain the maximum strength is a replacement level of 20% natural pozzolan. Moreover, it is reported that the effect of natural pozzolan on reducing the heat of hydration and combating sulfate attack was significant. Following the same path, Al-Swaidani (2017) investigated both the strength and durability of cement blended with ground volcanic scoria in the range of replacement levels of 10–35%. Durability-related properties such as water permeability, resistance to chloride penetration and porosity of concrete mixtures containing volcanic scoria as natural pozzolan up to 180 days were examined. It is summarized that scoria-based mixtures could achieve a similar strength to the plain concrete over time. Furthermore, the concrete mixtures with high content of scoria showed significant reduction in water and chloride permeability with lower porosity. Consequently, Elbar, Senhadji, Benosman, Khelafi, and Mouli (2018) studied the combined effect of curing conditions of elevated temperatures (20, 40, and 70 °C) on compressive and flexural strength of mortars and concrete with replacement levels of natural pozzolan in the range of 10–30%. The curing method at elevated temperatures increased the early-age strength and minimized the permeability to chloride. However, the later-age strength was negatively affected.

On the other hand, few researchers in recent years have directed their attention to the potential use of SR covering large area in the Arabian Peninsula as local sources of natural pozzolan for the production of durable concrete (Aldossari et al., 2019; Celik et al., 2014; Khan & Alhozaimy, 2011; Fares et al., 2017; Ozvan, Tapan, Onur, Tuba, & Depci, 2012). Therefore, an insight characterization on those type of ground SR is essential to interpret and assess their feasibility for use as alternative cementitious materials (ACMs) in concrete construction. A comparison between different researches on the use of SR as natural pozzolan in paste, mortar and concrete mixtures is summarized in Table 1.

The aim of this study is accordingly to generate physico-chemo-mechanical data on SR collected from different volcanic cones, which cover large areas in the Arabian shield (approximately 90,000 km^2). Accordingly, the difference in the performance of a variety of scoria rock samples procured from different regions in paste, mortar and concrete owing to ASTM C618 (2001) was explored and justified. This work is the first to cover samples procured from such large regions in this area of the study. A series of tests using different techniques to decipher the variation in SR physico-chemical properties and provide an insight into the fundamental parameters affecting their reactivity with cement and consequently the compressive strength. Various physical, mineralogical, and chemical properties of SR powders were determined using different techniques. These techniques included stereomicroscopy, X-ray fluorescence (XRF), X-ray diffraction (XRD), thermogravimetric (TG), and differential scanning calorimeter (DSC) analyses in addition to the use of field emission-scanning electron microscope (FE-SEM) analyses. Moreover,

Table 1. A comparison between various research studies on the use of natural pozzolan in construction.

Reference	Region	Optimized content	Observations
Shannag and Asim Yeginobali (1995)	**One region**, one sample was procured in Jordan	Up to 35%, effect of fineness on pozzolanic properties was investigated	Paste, mortar and concrete samples, increasing fineness increases the reactivity of natural pozzolan.
Rodriguez-Camacho and Uribe-Afif (2002)	**Different regions**, different samples were procured in Mexico	Up to 14%,*SAI with Portland cement ranges from 80.9% to 103.1% at 28 days	Pastes with cement and others with hydrated lime. They did not find a relation between main elemental oxide and natural pozzolans properties.
Turanli et al. (2004)	**Same region**, three different commercial types of natural pozzolans in Turkey	Investigated pozzolanic activity using strength of mortar containing 55% of natural pozzolans	Natural pozzolan with low content of main elemental oxides provided improved properties dependent on hardness and particle size distribution
Habert et al. (2008)	**Same region**, three natural pozzolanic deposits belonging to the Lafarge cement society	30%, studied the potential effect of the secondary minerals on the strength.	Mortar mixes, it is concluded that pozzolanic activity of natural pozzolans can be enhanced by a thermal treatment
Kaid et al. (2009)	**One region,** in Algeria	15–20%, pozzolanicity was investigated as a function of lime and natural pozzolan	Concrete mixtures, pozzolanicity was defined as a consumption of 18g portlandite per 100 g pozzolan
Cobîrzan et al. (2015)	**Three regions**, in Romania	25%, chemical reactivity and mineralogical content define pozzolanic reactivity	Paste mixes, the important criteria of selecting natural pozzolans for partial cement substitution in mortar and concrete are correlated with the chemical reactivity and mineralogical content.
Aldossari et al. (2019)	One region, different samples from same region in The Arabian Peninsula	20%, using remote sensing technique	In mortar, they concluded that the pozzolanic activity relies on the amorphous content in natural pozzolan
Current work	Three regions, different samples from each region were procured in The Arabian Peninsula	30%, development in the compressive strength was followed and pozzolanicity was investigated using thermal analysis.	Paste, mortar and concrete. It is concluded that the difference in pozzolanic reactivity relies on the mineralogical composition and amorphous content

*SAI = Strength activity index.

the use of thermal analyzer has enabled the quantification of pozzolanic reactivity of SR samples with cement.

2. Materials and testing protocol

2.1. Samples collection

A total number of 10 samples were procured from different volcanic cones (mountains) from three selected regions (R1, R2, and R3) along the Arabian shield. To summarize; three samples were procured from R1 and accordingly identified as R1S1, R1S2, and R1S3 while two samples from R2 were collected and identified as R2S1 and R2S2. Finally, five samples from R3 were collected and identified in the range from R3S1 to R3S5. Typical images of the selected volcanic cones from different regions R1, R2, and R3 with associated samples are shown in Figure 1.

Figure 1. SR samples collected from selected volcanic cones from the three identified regions.

Table 2. Location and nomenclature of the SR samples collected from three regions.

			GPS coordinates	
Region	Sample	Identification	Latitude (N)	Longitude (E)
R1	S1	R1S1	23°11.9103	39°56.9014
	S2	R1S2	23°12.271	39°56.2511
	S3	R1S3	23°13.5597	39°58.8020
R2	S1	R2S1	25°37.9160	37°73.0556
	S2	R2S2	25°37.7778	37°73.1667
R3	S1	R3S1	26°99.5833	42°24.5833
	S2	R3S2	27°05.4167	42°34.4440
	S3	R3S3	26°00.8056	42°34.2500
	S4	R3S4	26°91.7778	42°35.1389
	S5	R3S5	26°07.5000	42°36.1111

The locations of the selected regions for each sample were recorded and reported in Table 2 using the international GPS mapping system, which identifies the main coordinates of the field measurements. It is worth mentioning that these coordinates help the authors and other researchers to obtain the exact location of the samples in each region for coming plans and future studies. The full identification of each sample includes the GPS coordinates represented by latitude and longitude is summarized in Table 2. The projection of these coordinates was performed in the field using GPS on a Blackberry device and then finally plotted using Google's free service available on the Internet.

2.2. Characterization of scoria rocks

The effects of SR source on grindability, variations in the chemical and mineralogical compositions and other physical properties were assessed in this study. Prior to grinding, the procured SR grains were investigated using Leica EZ4 HD stereomicroscope and FE-SEM techniques. The grindability of the procured SR samples was evaluated by grinding each sample with initial sizes of $\leq$ 4 mm (as in Figure 1) for 120 minutes using FRITSCH Planetary Mono Mill Pulverisette grinding machine. After grinding, a thorough investigation was carried out on the procured samples. First, the particle size distributions (PSDs) of the ground samples, including the three main particle-size parameters (D10, D50, and D90), were determined using a laser PSD analyzer (LA 950V2, Horiba). The particle size parameters (D10, D50, and D90) obtained from the PSD analysis

represent the particle size diameters of which 10%, 50%, and 90% of the particle sizes in the tested powder were smaller than these corresponding diameters, respectively.

Second, XRF technique was used to obtain the chemical analysis of the samples. The elemental oxide composition was determined using a 2.4 kW PANalytical AXIOS XRF machine with pressed powder pellets made from approximately 12 g of sample. The crystalline structure of each SR sample was determined using XRD technique by PANalytical Empyrean diffractometer with CuKα radiation ($\lambda = 1.5406$ Å) operated at 45 kV and 40 mA. The scans were performed in the 2θ range from 5° to 65° with a scanning speed of 2° min^{-1}. XRD was used to investigate the main difference in the mineralogical phases of SR samples. Q600 thermal analyzer supported with simultaneous thermogravimetric analyzer (TGA) and DSC, from TA, was used to analyze the chemical reactivity of SR powders with cement in their pastes at 180 days. Sample weight was in the range of about 30 ± 5 mg of the cured paste sample after being dried and ground in an isolated chamber to minimize carbonation as much as possible. A nitrogen gas flow of 50 ml/min was applied during heating of the tested sample from room temperature to 1100 °C at a heating rate of 20 °C/min. The collected data from the weight loss and the accompanied heat flow were plotted to obtain TGA and DSC curves, from which the amount of remained portlandite (hydrated lime, calcium hydroxide (CH)) in paste sample can be estimated.

2.3. Characterization of SR mortars

Control and SR mortar mixtures were prepared using ordinary Portland cement (PC) (ASTM C150, 2012) and SR (after a grinding time of 120 minutes) as binder materials for the determination of strength activity index (SAI) and the use in concrete mixtures. The SAI was determined according to ASTM C311 test procedures (ASTM C311, 2007). The control (Co) mixture was prepared with 100% PC whereas the SR-based mortar mixtures incorporated 20% SR as partial PC replacement materials (on a weight basis). SR mixtures were designated owing to the identification given in Table 2. All mortar mixtures were prepared with water-to-binder (W/B) ratio of 0.5 of sand/binder ratio of 2.75 and normally cured for up to 180 days. The average compressive strength of 3 samples ($50 \times 50 \times 50$ mm mortar cubes) from each mixture was determined at curing ages of 28 and 180 days. Each SAI value represents the ratio, in percentage, of the average strength of SR mixture to that of the control. FE-SEM was used to assess the microstructure and hydration progress of similar cement pastes prepared with W/B ratio of 0.5 and left to hydrate up to 180 days. Small pieces of freshly broken samples were collected at this age to assess the microstructural features in each mixture using FE-SEM. As well, the remained amount of CH relative to that in the control sample was estimated using Q600 thermal analyzer for the same freshly broken, dried and ground samples in an isolated chamber.

2.4. Performance of SR in concrete mixtures

To evaluate the performance of SR, concrete mixtures with 30% SR as cement replacement by weight were compared with control mixture. The selection of 30% SR was proposed to investigate the potential of using this acceptable amount to promote SR application in concrete industry. Coarse and fine aggregates were used to prepare concrete mixtures. A blend of two sizes of calcareous aggregates, namely 10 and 20 mm (C10 and C20, respectively), complying with ASTM C33 (2007), were used as coarse aggregates with specific gravities of 2.63 and 2.62, respectively. The fine aggregates were also a blend of 35% crushed sand and 65% natural sand (CS and NS, respectively), complying with ASTM C33 (2007) with specific gravities of 2.65 and 2.59, respectively. Sieve analysis of fine and coarse aggregate in addition to their combined grading is shown in Figure 2. The details of mix proportions are presented in Table 3. Six cube samples of $100 \times 100 \times 100$ mm were cast and tested for compressive strength in accordance with BS 1881,

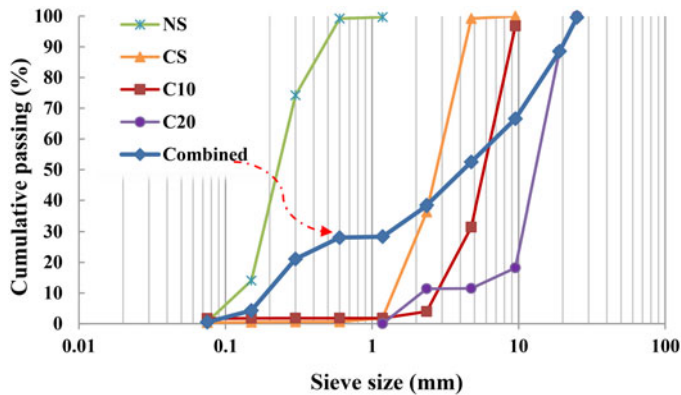**Figure 2.** Sieve analysis of fine and coarse aggregates used in concrete including combined gradation of all aggregates in concrete.

Table 3. Mix proportion of the tested mixes (kg/m³).

Ingredients	Control (Co)	30% SR
Cement	350	245
SR	0	105
Coarse aggregate 20 mm	735	735
Coarse aggregate 10 mm	315	315
Crush sand	270	270
Natural sand	510	510
Water	175	175

1881 (1986). First, the samples were kept under a laboratory environment for the first 24 hours. After that, the specimens were demolded and placed in a lime-saturated water tank until testing times of 28 and 90 days.

3. Results and discussion
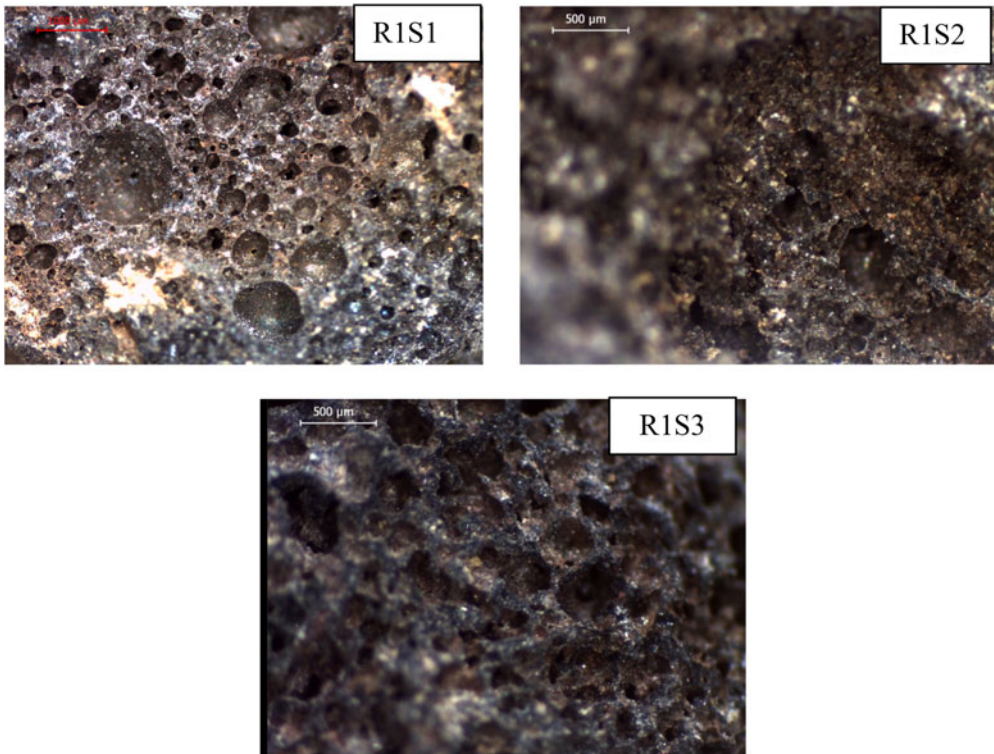
3.1. Physical analysis

Grinding of SR into fine powder is a key step in processing and preparation of SR for an effective use as natural pozzolanic material in concrete. In general, the characteristic features of SR samples include low dense and porous lightweight structure that lead to an easy grinding. The ASTM C618 (2001) specified a maximum of 34% residue on 45-μm sieve to use as a pozzolan. The main reason is that the particles with sizes over 45 microns are considered as a non-reactive and behave like concrete filler. The three main size parameters (D10, D50, and D90) obtained from PSD analysis of tested PC and SR powders after a grinding time of 120 min are shown in Table 4. Due to the absence of the characteristic features of SR in R3S1 and R3S3, they were excluded from further investigation as they were difficult to grind, as demonstrated in Figure 3. Based on PSD analysis, the tested SR powders have satisfied the maximum residue content specified by ASTM C618 (2001). All ground SR powders proved finer than cement based on the main size parameters listed in Table 4.

Data in Table 4 indicate that the grindability of both R1S3 and R2S1 was the highest with respect to the rest of SR samples whereas the grindability of R3S4 and R2S2 was the lowest. The variation in grindability among the various samples could be explained by the difference in the structures of the vesicular textures of SR gains. In addition, the initial strength of the bridges connecting the vesicles inside the grains was another determining factor. The stereomicroscopy analysis of SR samples collected from the three regions (R1, R2, and R3) shows the vesicular

Table 4. The main particle size parameters of SR samples after 120 min of grinding (D10, D50 and D90).

Passing (μm)	R1			R2		R3					
	R1S1	R1S2	R1S3	R2S1	R2S2	R3S1	R3S2	R3S3	R3S4	R3S5	PC
D10	0.3	0.3	0.3	0.3	0.4	NA	0.3	NA	0.3	0.3	2
D50	4.6	5.4	2.0	3.2	5.7	NA	4.9	NA	5.8	4.7	15
D90	24.7	24.6	18.6	17.2	25.0	NA	21.6	NA	25.9	23.2	50

NA: Not applicable due to the grinding difficulty.

Figure 3. Difficult grindability shown by R3S3.

Figure 4. Stereomicroscopy images of SR from R1.

textures in each SR sample and the bridges connecting the vesicles, as depicted in Figures 4–7. It is shown that samples from region R1 are characterized by the presence of air bubbles of different sizes in a dense structure. These variations might be attributed to the presence of
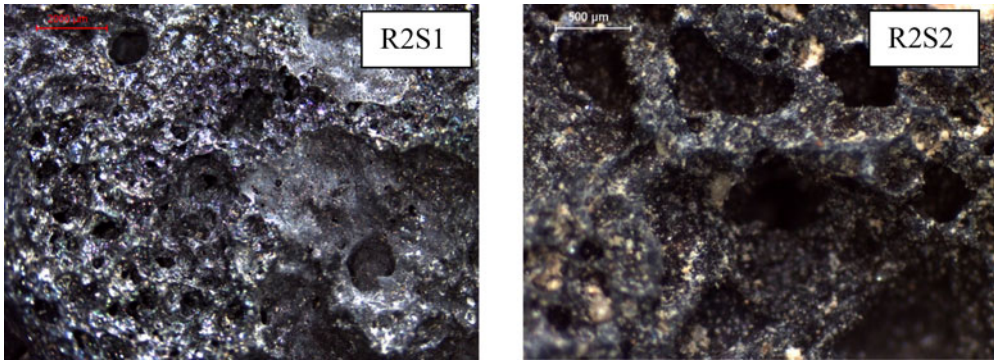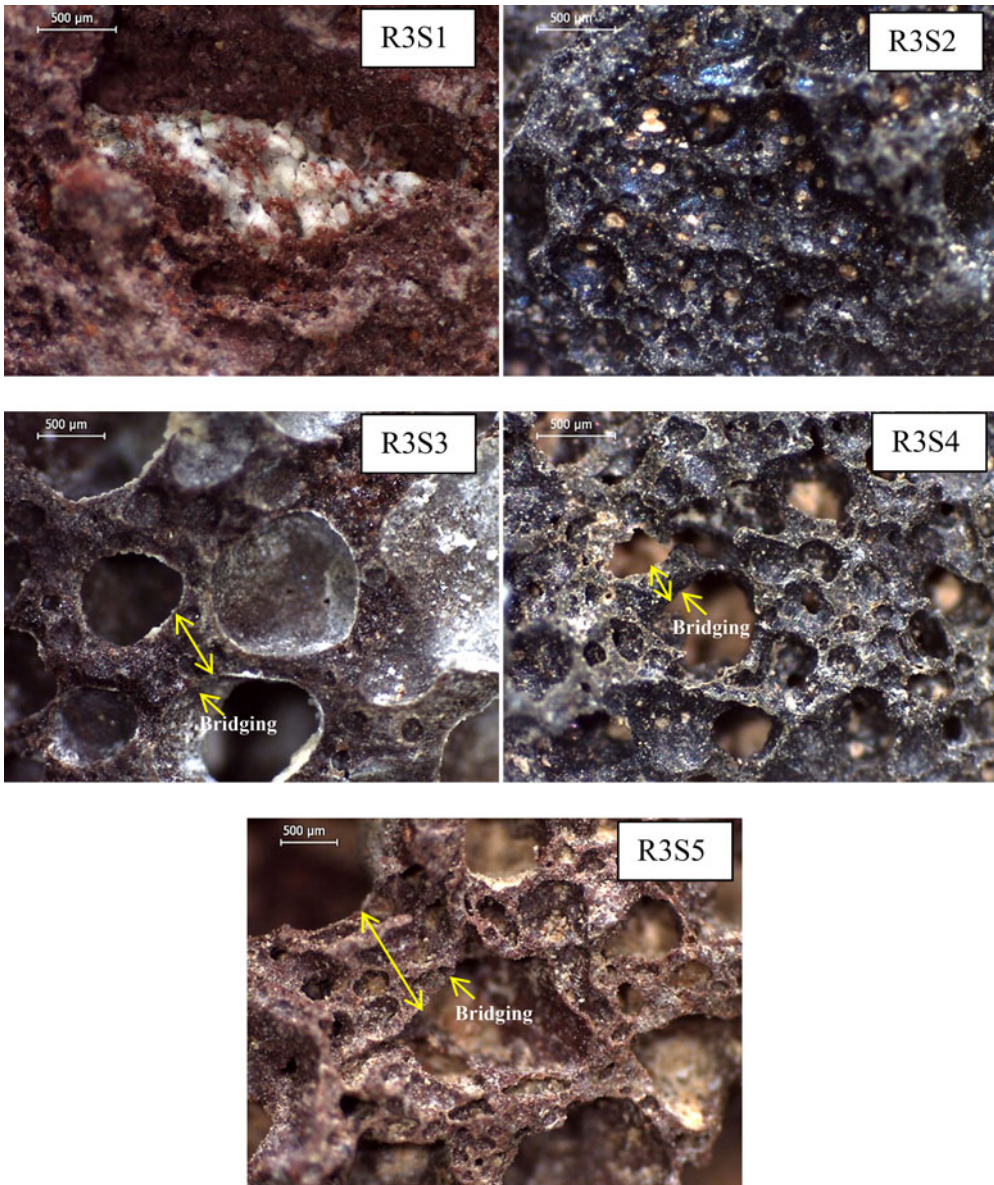
Figure 5. Stereomicroscopy images of SR from R2.

Figure 6. Stereomicroscopy image of different SRs from R3.
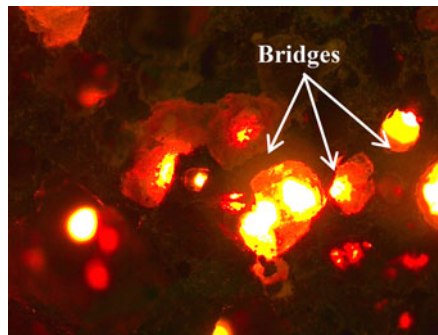
Figure 7. Microscopic investigation of SR samples using light-pores interaction to visualizing the bridging effect and connectivity of pores.

different phases and minerals of different thermal properties, as can be verified from XRD analysis. R1S1 and R1S3 showed a sintered, dense and coarse structure whereas R1S2 showed a sintered but less dense and fine structure, as demonstrated in Figure 4. Stereomicroscopy images of R2S1 and R2S2 samples collected from region R2 are presented in Figure 5 where they have been shown to be characterized by the presence of small to very fine air bubbles, which make them less dense.

Stereomicroscopy images of samples collected from region R3 (R3S1, R3S2, R3S3, R3S4 and R3S5) are presented in Figure 6. These samples are characterized by different colors and pore sizes due to the weathering effects. R3S1 shows a sintered, non-porous and hard structure, while R3S2 shows a sintered and fine structure with enclosed quartz grains. The stereomicroscopy image of R3S3 shows a sintered, coarse and hard structure with very large pores whereas R3S4 and R3S5 show sintered, coarse structures with large pores, as given in Figure 6.

It is believed that the pore network in SR leads to a bridge-like structures, as clearly shown in Figure 6. Accordingly, the strength of these bridges defines the initial energy required to break and accelerate the effective grinding process. Microscopic investigation of SR samples using the technique of interaction of pores with incident light to visualizing the bridging effect due to pore network connection was conducted. The interaction of incident light with bridges shows the actual thickness of each pore and reflect the bridging effect in SR grain, as shown in Figure 7. This type of analysis is promising and provides significant information about the connected pores that control the grindability of SR samples. It should be highlighted that this part of the analysis requires further investigation to correlate grindability with different sources of light.
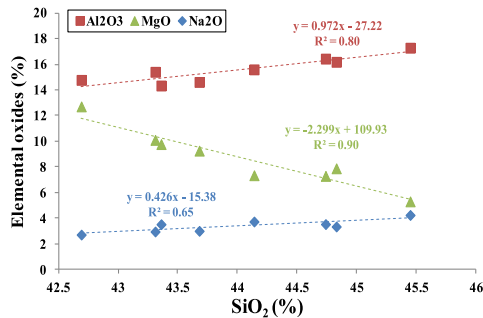
3.2. Chemical analysis

The XRF analysis of PC and SR powders is summarized in Table 5. Each value in this table represents the average of duplicate measurements, which have a negligible difference reflecting the homogeneity of SR powders. The ASTM C618 (2001) requirements mandate that the sum of the main elemental oxides (SiO_2, Al_2O_3 and Fe_2O_3) should be $\geq$ 70% (ASTM C618, 2001) for Class N pozzolans. The chemical analysis of the collected samples confirmed their satisfaction to ASTM C618 requirements, except for R3S4 sample, which was at the borderline. R2S1 sample exhibited the highest sum of main oxides (77.3%), whereas R3S4 exhibited the lowest one (69.4%), as reported in Table 5. It is worth to remind that ASTM C618 (2001) requirements mandate that SO_3 should not be > 4% and loss on ignition (L.O.I.) should not be > 10%. From the chemical analysis presented in Table 5, it is confirmed that SR powders have satisfied the requirements of ASTM C618 (2001) for SO_3 and L.O.I. in pozzolans.

Important relationships between elemental oxides analysis and physical properties of SR samples have been explored and established in this part of the study. The most abundant elemental

Table 5. Chemical analysis of different SR powders from different regions.

| | R1 | | | R2 | | R3 | | | |
Oxides (%)	R1S1	R1S2	R1S3	R2S1	R2S2	R3S2	R3S4	R3S5	PC
SiO_2	43.31	42.69	44.83	45.45	44.74	43.36	43.68	44.14	20.41
Al_2O_3	15.41	14.78	16.19	17.29	16.44	14.34	14.62	15.6	5.32
Fe_2O_3	12.48	12.65	11.97	14.54	12.96	12.94	11.09	11.91	4.1
CaO	9.26	9.13	8.53	7.53	9.64	8.75	9.66	9.62	64.14
MgO	10.1	12.71	7.88	5.3	7.29	9.77	9.26	7.34	0.71
SO_3	0.06	0.05	0.05	0.11	0.06	0.41	0.07	0.11	2.44
P_2O_5	0.4	0.3	0.48	0.5	0.4	0.64	0.5	0.47	0.04
TiO_2	2.19	1.99	2.23	2.77	2.19	2.54	2.1	2.23	0.3
MnO	0.19	0.17	0.17	0.2	0.19	0.21	0.16	0.19	0.07
Na_2O	2.95	2.71	3.34	4.24	3.53	3.52	3	3.73	0.1
K_2O	0.75	0.55	0.96	1.1	0.94	1.58	1.53	1.46	0.17
Cl	0.03	0.03	0.07	0.05	0.1	0.07	0.09	0.05	0.01
Cr_2O_3	0.12	0.16	0.09	0.1	0.11	0.1	0.09	0.09	–
L.O.l	0.95	0.45	1.9	0.58	1.21	1.51	2.33	2.82	2.18
$\Sigma\ (SiO_2+Al_2O_3+Fe_2O_3)$	71.1	70.1	73.0	77.3	74.1	70.6	69.4	71.7	NA

Figure 8. Relationship among different elemental oxides.

oxide in SR samples is SiO_2 followed by Al_2O_3 and Fe_2O_3. SiO_2 was taken as the main elemental oxide and a reference to which different correlations with other elemental oxides can be established. It is confirmed that an increase in SiO_2 content leads to an obvious increase in alumina and sodium oxide contents along with a decrease in magnesia content, as shown in Figure 8. These findings point out to the formation of sodium-rich alumino silicate compounds (as in albite) in the presence of calcium, which can be confirmed using XRD analysis. Previous studies have indicated that the formation of sodium aluminosilicate compounds favors the reduction in magnesia content (Boyanov, 2005), which can also be confirmed using XRD analysis. As well, an increase in sodium content (Na_2O) appears to be accompanied by an increase in the amount of SiO_2 and Al_2O_3 that melted in the structures of SR samples to form sodium aluminoslilicates. The microstructure elemental mapping analysis shows the effect of iron (Fe)-bearing minerals forming sheath that covers aluminosilicate network. This sheath affects network quality and thus inhibits or slows down the rate of pozzolanic activity of R2S2 sample, as shown in Figure 9. On the other hand, it is obviously depicted that the iron-bearing minerals are distributed in scattered and low dense manner at the surface of R3S4 particle. Thus, aluminosilicate network becomes in a direct subjection or contact with surroundings; accordingly, a higher pozzolanic activity is expected in this sample.

3.3. Mineralogical analysis

Mineralogical analysis of SR samples is shown in Figure 10. The results of XRD analysis reveal a significant amount of an amorphous glass phase presents in all SR samples. The presence of
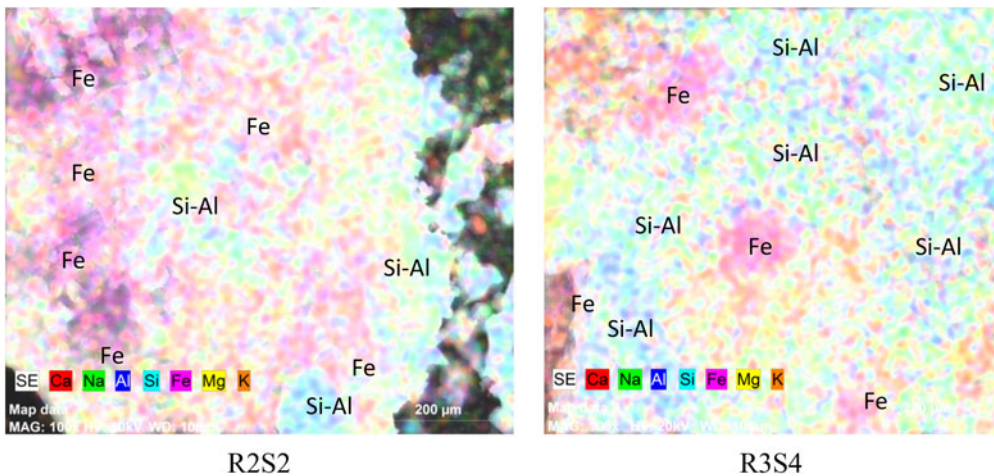
Figure 9. Microstructural elemental mapping analysis of ground R2S2 and R3S4 particles using overlapping mode.
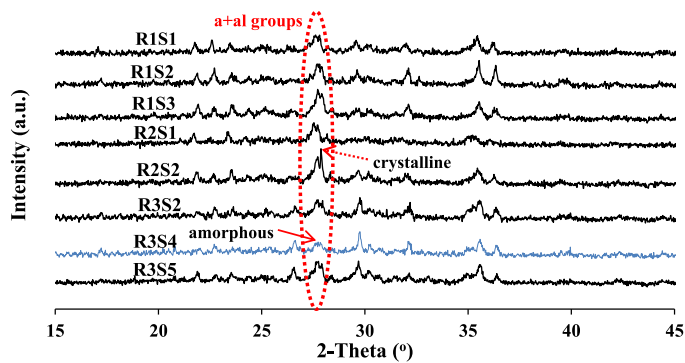

Figure 10. XRD analysis of SR samples (a = Anorthite; al = Albite).

different mineralogical compositions was inferred from XRD analysis as well. The glassy phase seems to be higher in the samples collected from R3 region due to the higher halo of pozzolanicity, as demonstrated in Figures 10 and 11. Interpreted XRD patterns of the typical main peaks of two SR samples (R2S1 and R3S4) are illustrated in Figure 11. The analysis shows that SR samples contain pyroxene (augite, diopside and enstatite), olivine (frosterite) and feldspars plagioclase (albite and anorthite) minerals. Accordingly, anorthite (Ca-Al silicate), albite (Na-Al silicate), enstatite (Mg silicate), augite (Ca-Fe-Mg silicate), diopside (Ca-Mg-Fe silicates), frosterite (Mg-Fe silicates) and quartz are the main minerals whose primary peaks vary notably in SR samples from regions R1 and R2. Therefore, it is expected that the nature of these minerals might affect the pozzolanic activity of SR samples. On the other hand, augite and diopside (CA-Fe-Mg and Ca-Mg-Fe silicates, respectively) are mostly found in region R3 samples.

The minerals found in SR samples procured from R1 and R2 regions have higher crystallinity than those in the samples from R3. Therefore, the degree of crystallinity is higher in R1 and R2 than in R3. Albite-anorthite groups predominantly found in R1 and R2 samples have higher crystallinity than those in R3 samples and especially in R3S4. Therefore, it can be initially concluded that sodium aluminosilicate minerals appear in amorphous state in R3S4 sample while the other samples are shown to have these minerals with a higher degree of crystallinity. Therefore, the variation in the pozzolanic activity is expected to vary dependent on the ratio of crystalline phase to amorphous phase exist in SR. As well, pozzolanic activity relies on the chemical nature
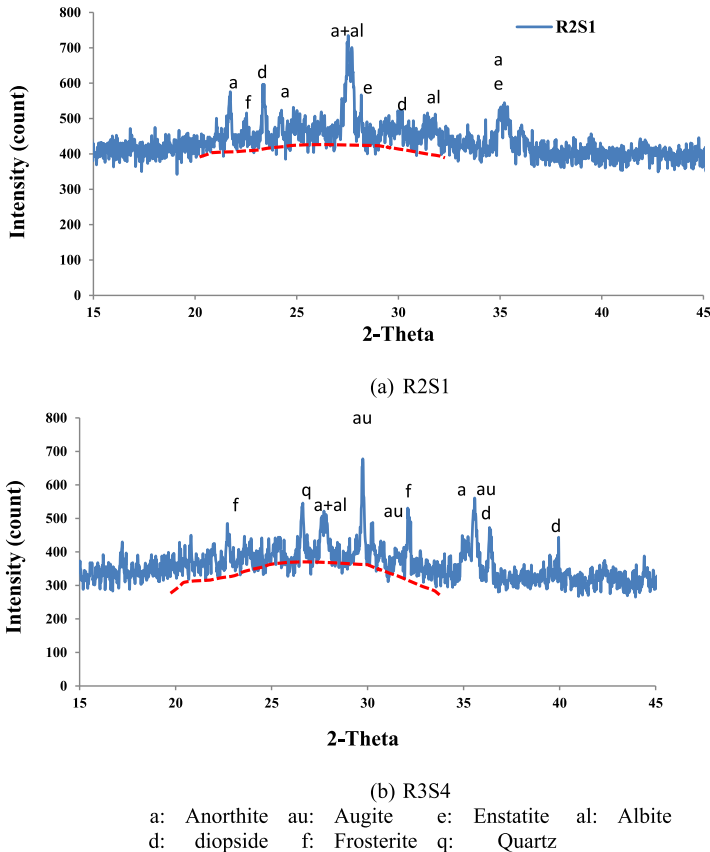
Figure 11. XRD analysis of (a) R2S1 and (b) R3S4 as a general example.

of SR composition i.e. content of elemental oxides, especially of iron oxides and their mineralogical nature.

3.4. Variation in strength activity index (SAI)

SAI is an important evaluation criterion for the performance of pozzolans in mortar and concrete. Selected SR samples (R1S1, R2S1, R3S2, and R3S4) were used to investigate and correlate the variation in mineralogical composition to the pozzolanic activity over time. The SAI values of the investigated SR mortar mixtures containing R1S1, R2S1, R3S2, and R3S4 at curing ages of 28 and 180 days are shown in Figure 12. The R3S4 mixture shows the highest SAI values at 28 and 180 days of approximately 80% and 93%, respectively. The mixtures R2S1 and R3S2 have similar SAI values at 28 and 180 days in the range of 77–82%, as shown in Figure 12. The mixture R1S1 has given SAI values of 72% and 77% at 28 and 180 days, respectively. Moreover, the results of SAI could not be correlated with the sum of the main elemental oxides ($SiO_2+Al_2O_3+Fe_2O_3$) shown in Table 5 similar to the work reported by Rodrıguez-Camacho and Uribe-Afif (2002).

To explain, R3S4 whose sum of the main elemental oxides was the lowest, it has however yielded the highest strength activity index. On the other hand, R2S1 whose sum of main oxides was the highest has provided an average SAI value. The highest pozzolanic activity of R3S4 is construed to its higher amorphous content, as indicated by XRD analysis. Moreover, albite minerals (sodium aluminosilicate) are shown to exist in the amorphous state. Therefore, combination of XRD patterns along with mineralogical composition enables reasonable assessment and
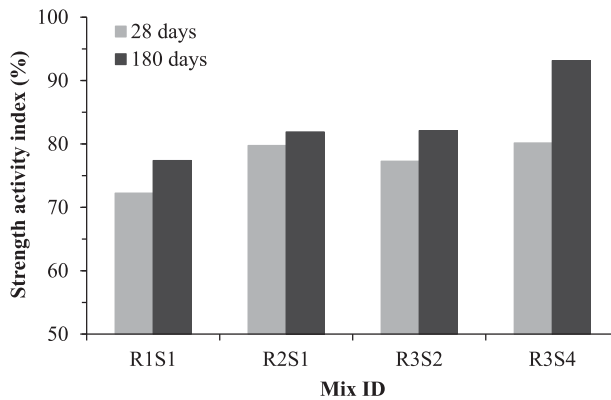
Figure 12. Strength activity index of SR samples procured from different regions.

prediction of the pozzolanic activity of SR samples. The amorphicity of albite-anorthite minerals can be taken as a mineralogical index of pozzolanic activity of SR.

3.5. FE-SEM analysis of hydrated SR pastes

The microstructure development of the hydrated paste mixtures of control (Co), R1S1, R2S1, R3S2, and R3S4 prepared with W/B ratio of 0.5 were evaluated at a curing age of 180 days. The microstructural analyses of these paste mixtures were carried out using FE-SEM. The results of FE-SEM analysis of freshly broken pieces from cement pastes of Co, R1S1, R2S1, R3S2 and R3S4 mixtures are shown in Figure 13. The microstructural analysis of the pastes reveals the presence of ettringite crystals and calcium silicate hydrate (C–S–H) in the control mixture. Similar to control, R1S1 mixture shows the presence of ettringite needles (of smaller size), C–S–H and monosulfoaluminate (AFm) hexagonal crystals of lamellar structure. The mixture R2S1 shows the presence of C–S–H and noticeable occurrence of ettringite needles that is attributed to the sulfate contamination in the original R2S1 sample. The microstructural analysis of the mixture R3S2 shows the presence of C–S–H and the reaction rim formation around SR particles, as an indication to the continuation of the hydration reaction from the periphery of SR particles inwards. Similarly, the mixture with R3S4 shows the presence of two types of microstructure, i.e., amorphous and fibrous-like C–S–H structures, which explain the improvement in the compressive strength at a curing age of 180 days. Therefore, the poly-phase structure including amorphous albite (Na-Al silicate) in R3S4 sample has an improving effect on its cementitious properties. Amorphous albite-phase reaction with alkalis in pore water in cement paste leads to the formation of geopolymeric-like structures, as clearly presented in Figure 13.

3.6. XRD analysis of hydrated SR pastes

The mineralogical compositions of the investigated SR paste mixtures were obtained using XRD technique as shown in Figure 14. The presence of CH, ettringite (AFt), and C–S–H gel formation is confirmed in all mixtures. The highest intensity of CH peak is found in the control mixture. R1S1 mixture has shown the presence of AFm and AFt with the highest intensities. The lowest intensities of CH, AFt and AFm are present in R3S4 mixture. These results are in a good agreement with FE-SEM analysis, which confirms the pozzolanic activity of R3S4 sample. The presence of additional C–S–H, which has a tobermorite-like structure in R3S4 mixture, is also confirmed, as in Figure 14. This finding agrees with the results from FESEM analysis.
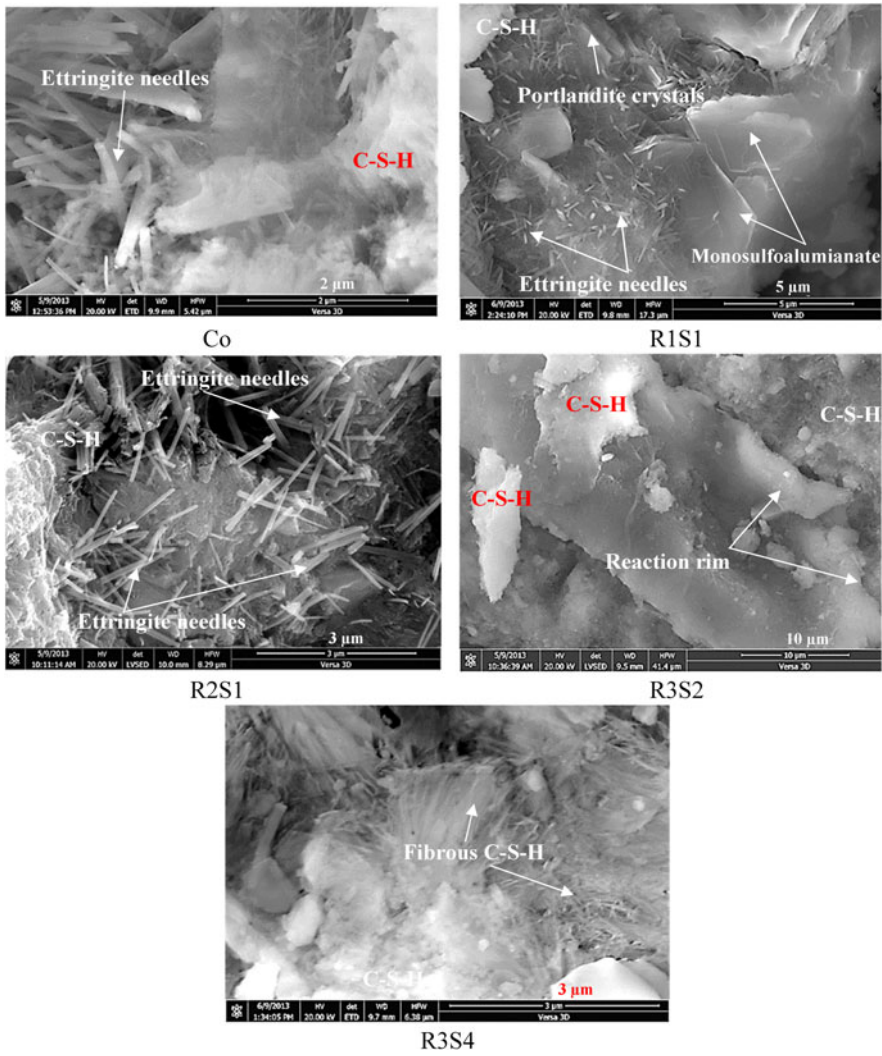
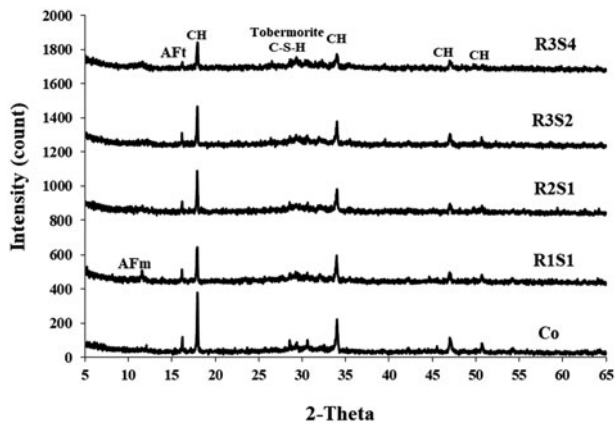**Figure 13.** FESEM photomicrographs of the paste mixtures (Co, R1S1, R2S1, R3S2, and R3S4) at a curing age of 180 days.

Figure 14. XRD analysis of NP paste mixtures at a curing age of 180 days.

3.7. DSC/TGA analyses of hydrated SR pastes

DSC/TGA thermal analyses were carried out on the same powders of the paste mixtures and the results are shown in Figures 15 and 16, respectively. The estimated amount of the remained CH is summarized in Table 6. DSC analysis shown in Figure 15 confirms that R3S4 mixture is characterized with an obvious endothermic peak at approximately 150 °C, which might be attributed to the dehydration of interlayer water in C–S–H, ettringite, monosulphate and/or carboaluminate hydrates (Kaminskas, 2006). The obvious endothermic peak at 105–200 °C presents only in R3S4 sample, which is strongly ascribed to the thermal decomposition of tobermorite-like C–S–H (Alhozaimy, Fares, Al-Negheimish, & Jaafar, 2013). A sharp endothermic peak appears in the range of 400 to 500 °C in all mixtures, which is attributed to CH phase (Pourkhorshidi, Najimi, Parhizkar, Jafarpour, & Hillemeier, 2010). Another weak endothermic peak in the range of 700 to 750 °C is almost found in all mixtures. This endothermic peak is attributed to the presence of calcite as a minor contaminant in SR. Part of it might also be attributed to the thermal decomposition of AFt due to the structural –OH and –SO$_3$ groups. The amount of CH remained in each mixture in the range of 400 to 500 °C could be estimated quantitatively from TG analysis shown
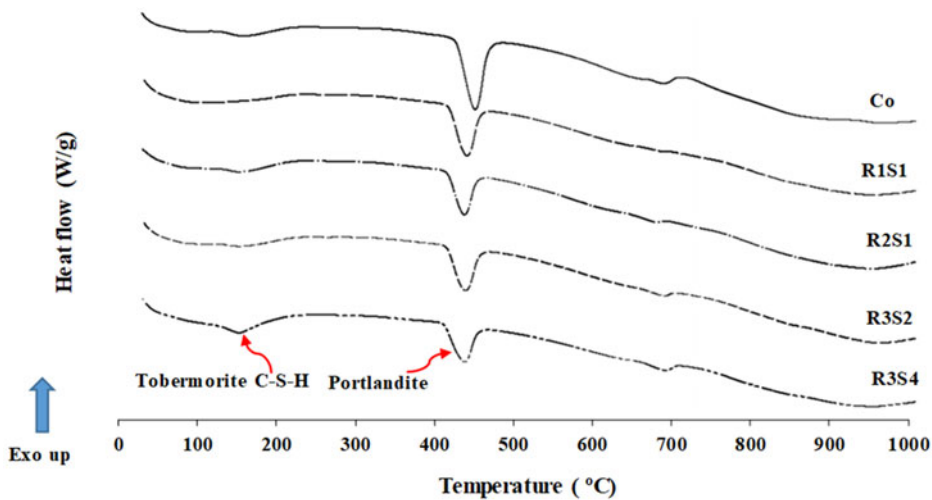

Figure 15. Differential scanning calorimeter (DSC) of different SR cement paste mixtures at a curing age of 180 days.
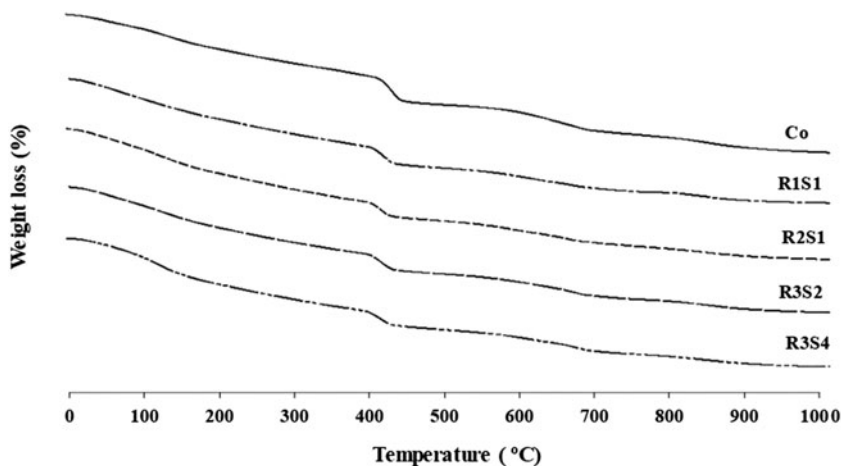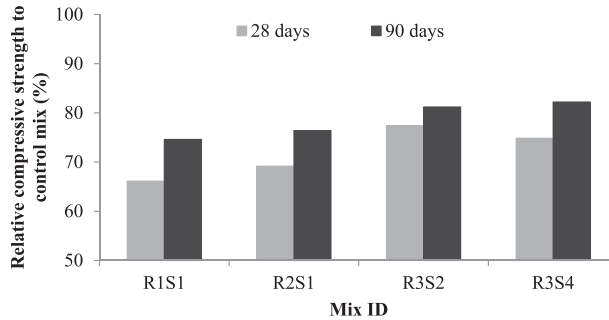

Figure 16. Thermogravimetric analysis (TGA) of different SR cement paste mixtures at a curing age of 180 days.

Table 6. Amount of CH remained in SR mixtures calculated using TG analysis.

Mixtures A	Amount of remained CH (%)
Co	100
R1S1	80
R2S1	76
R3S2	75
R3S4	71

Figure 17. Relative compressive strength of SR samples procured from different regions to control mix.

in Figure 16 and listed in Table 6. The effect of replacement level has been taken into account while calculating the relative amount of CH remained in the paste mixtures. The amount of CH remained in the mixtures with respect to that in the control one can be taken as another index of the pozzolanic activity of SR samples. The TG analyses confirm the pozzolanic activity of R3S4 sample collected from region R3. These results are in a good agreement with the previous data from FESEM and XRD analyses. The values indicated in Table 6 refer to the presence of a critical CH consumption value seems to be at 25% after which an obvious increase in the corresponding compressive strength can be noted as the case with R3S4. Therefore, the pozzolanic activity of SR is due to a chemical reaction with portlandite and not to a physical filling effect.

3.8. Evaluation of SR performance in concrete mixtures

Figure 17 shows the effects of SR (R1S1, R2S1, R3S2, and R3S4) on the compressive strength of their concrete mixtures with respect to the control mixture. All SR concrete mixtures displayed lower compressive strengths than the control at all curing ages; however, they showed gradual improvement in strength with time. For instance, at 28 days, the relative compressive strength of SR mixtures has ranged from 66 to 75% compared to the control mixture. On the other hand, the relative compressive strength of SR mixture has ranged between 74 and 82% at 90 days. The reduction in compressive strength is due to the dilution effect of PC with 30% SR while the improvement in the strength was attributed to the pozzolanic activity of SR. Therefore, curing time of SR concretes plays an important role in improving the mechanical properties, as the case with most of pozzolanic materials. In addition, the results of compressive strength of concrete mixtures revealed that R3S2 and R3S4 concrete mixtures provide the highest compressive strengths compared with R1S1 and R2S1 at all testing ages. The development in compressive strength of R3S2 and R3S4 concrete mixtures was construed to the pozzolanic reaction, which has led to a cementitious matrix with enhanced microstructure. SR samples can be deemed as pozzolanic materials rather than being considered as just fillers. The research work performed in this study could correlate the mechanical properties to the mineralogical composition similar to the work performed by Habert, Choupay, Montel, Guillaume, and Escadeillas (2008) and

Cobîrzan, Balog, and Moşonyi (2015). Moreover, the effect of iron-bearing mineral in minimzing the pozzolanic reactivity has been highlighted in the current research. In comparison with the data reported in Table 1, it could be concluded that the current research work has conducted most of the reported tests in a single research work. In addition, both the enhancement and reduction in strength of mortar and concrete due to SR as per the region and physico-chemical properties could be successfully justified.

4. Conclusions

Based on the results of this investigation, the following conclusions can be drawn:

1. Combination of characterization tests listed in this research have contributed in the interpretation and assessment of SR pozzolanic activity for use as an alternative supplementary cementitious material in concrete.
2. The pozzolanic activity of SR expressed by SAI did not correlate well with the sum of the main elemental oxides ($SiO_2+Al_2O_3+Fe_2O_3$). However, R3S4 has given the highest SAI value despite its lowest sum of the main elemental oxides. This was attributed mainly to the mineralogy of silicate phase referred to as the proportion of amorphous albite-anorthite minerals to diopsite-augite minerals. This proportion seems to be one of the main parameters affecting the pozzolanic activity of SR.
3. Thermal analysis has confirmed that the pozzolanic activity of SR samples is in a good agreement with SAI results. Therefore, the enhancement effect is due to pozzolanic activity not to the filling effect.
4. The amorphous sodium aluminosilicate is the predominant form of minerals in R3S4 sample. Crystalline calcium iron-magnesium silicates are found in all samples in a way that refers to their role in inhibiting the pozzolanic activity of SR.
5. Tobermorite-like C–S–H was the main hydration phase formed in R3S4 sample, which is considered as the main responsible for a relatively high pozzolanic activity.
6. The high strength activity index of R3S4 was further confirmed using concrete mixtures validating the current approach of the effect of proportion of silicate phases on pozzolanic activity. Therefore, the general conclusion is that SR samples act as a pozzolanic material not as a filler only.

Disclosure statement

No potential conflict of interest was reported by the authors.

Funding

ORCID

Galal Fares 🔟 http://orcid.org/0000-0003-1241-4772

References

Aldossari, M. S., Fares, G., & Ghrefat, H. A. (2019). Estimation of pozzolanic activity of scoria rocks using ASTER remote sensing. *Journal of Materials in Civil Engineering*, *31*(7), 04019100. doi:10.1061/(ASCE)MT.1943-5533.0002734

Alhozaimy, A., Fares, G., Al-Negheimish, A., & Jaafar, M. S. (2013). The autoclaved concrete industry: An easy-to-follow method for optimization and testing. *Construction and Building Materials*, 49, 184–193. doi:10.1016/j.conbuildmat.2013.08.024

Al-Swaidani, A. M., & Aliyan, S. D. (2015). Effect of adding scoria as cement replacement on durability-related properties. *International Journal of Concrete Structures and Materials*, 9(2), 241–254. doi:10.1007/s40069-015-0101-z

Al-Swaidani, A. M. (2017). Production of more durable and sustainable concretes using volcanic scoria as cement replacement. *Materiales de Construcción*, 67(326), 118. doi:10.3989/mc.2017.00716

ASTM C150 (2012). *Standard specification for Portland cement*. West Conshohocken, PA: ASTM International.

ASTM C311 (2007). *Standard test methods for sampling and testing fly ash or natural pozzolans for use in Portland-cement concrete*. West Conshohocken, PA: ASTM International.

ASTM C33 (2007). *Standard specification for concrete aggregates*. West Conshohocken, PA: ASTM International.

ASTM C618 (2001). *Standard test methods for coal ash and raw or calcined natural pozzolan for use as a mineral admixture in concrete*. West Conshohocken, PA: ASTM International.

Boyanov, B. (2005). Solid state interactions in the systems CaO (CaCO$_3$)-Fe$_2$O$_3$ and CuFe$_2$O$_4$-CaO. *Journal of Mining and Metallurgy, Section B: Metallurgy*, 41(1), 67–77. doi:10.2298/JMMB0501067B

BS 1881 (1986). *Testing concrete. Method for determination of compressive strength of concrete cubes*. London, UK: British Standards Institution.

Cavdar, A., & Yetgin, S. (2007). Availability of tuffs from northeast of Turkey as natural pozzolan on cement, some chemical and mechanical relationships. *Construction and Building Materials*, 21(12), 2066–2071. doi:10.1016/j.conbuildmat.2006.05.034

Celik, K., Jackson, M., Mancio, M., Meral, C., Emwas, A.-H., Mehta, P., & Monteiro, P. (2014). High-volume natural volcanic pozzolan and limestone powder as partial replacements for Portland cement in self-compacting and sustainable concrete. *Cement and Concrete Composites*, 45, 136–147. doi:10.1016/j.cemconcomp.2013.09.003

Cobîrzan, N., Balog, A.-A., & Moşonyi, E. (2015). Investigation of the natural pozzolans for usage in cement industry. *Procedia Technology*, 19, 506–511. doi:10.1016/j.protcy.2015.02.072

Colak, A. (2003). Characteristics of pastes from a Portland cement containing different amounts of natural pozzolan. *Cement and Concrete Research*, 33(4), 585–593.

Elbar, E., Senhadji, Y., Benosman, A. S., Khelafi, H., & Mouli, M. (2018). Effect of thermo-activation on mechanical strengths and chlorides permeability in pozzolanic materials. *Case Studies in Construction Materials*, 8, 459–468. doi:10.1016/j.cscm.2018.04.001

Fares, G., Alhozaimy, A., Alawad, O. A., & Al-Negheimish, A. (2017). Properties of high-performance concrete incorporating high-volume ground scoria rocks as natural pozzolan. *Magazine of Concrete Research*, 69(14), 703–715. doi:10.1680/jmacr.15.00420

Habert, G., Choupay, N., Montel, J. M., Guillaume, D., & Escadeillas, G. (2008). Effects of the secondary minerals of the natural pozzolans on their pozzolanic activity. *Cement and Concrete Research*, 38, 963–975. doi:10.1016/j.cemconres.2008.02.005

Hossain, K. M. A. (2006). Blended cement and lightweight concrete using scoria: Mix design, strength, durability and heat insulation characteristics. *International Journal of Physical Sciences*, 1(1), 5–16.

Kaid, N., Cyr, M., Julien, S., & Khelafi, H. (2009). Durability of concrete containing a natural pozzolan as defined by a performance-based approach. *Construction and Building Materials*, 23(12), 3457–3467. doi:10.1016/j.conbuildmat.2009.08.002

Kaminskas, R. (2006). The effect of pozzolana on the properties of the finest fraction of separated Portland cement. Part 1. *Ceramics – Silikáty*, 50(1), 15–21.

Khan, M. I., & Alhozaimy, A. M. (2011). Properties of natural pozzolan and its potential utilization in environmental friendly concrete. *Canadian Journal of Civil Engineering*, 38(1), 71–78. doi:10.1139/L10-112

Moufti, M., Sabtan, A., El-Mahdy, O., & Shehata, W. (1999). Preliminary Geologic and Engineering Assessment of the Pyroclastic Deposits in the Central Part of Harrat Rahat. *Journal of King Abdulaziz University-Earth Sciences*, 11(1), 59–88. doi:10.4197/Ear.11-1.4

Moufti, M. R., Sabtan, A. A., El-Mahdy, O. R., & Shehata, W. M. (2000). Assessment of the industrial utilization of scoria materials in central Harrat Rahat, Saudi Arabia. *Engineering Geology*, 57(3-4), 155–162. doi:10.1016/S0013-7952(00)00024-7

Ozvan, A., Tapan, M., Onur, E., Tuba, E., & Depci, T. (2012). Compressive strength of scoria added Portland cement concretes. *Gazi University Journal of Science*, 25(3), 769–775.

Pourkhorshidi, A. R., Najimi, M., Parhizkar, T., Jafarpour, F., & Hillemeier, B. (2010). Applicability of the standard specification of ASTM C 618 for evaluation of natural pozzolans. *Cement and Concrete Composites*, 32, 794–800. doi:10.1016/j.cemconcomp.2010.08.007

Rodrıguez-Camacho, R. E., & Uribe-Afif, R. (2002). Importance of using the natural pozzolans on concrete durability. *Cement and Concrete Research*, 32, 1851–1858. doi:10.1016/S0008-8846(01)00714-1

Senhadji, Y., Escadeillas, G., Khelafi, H., Mouli, M., & Benosman, A. S. (2012). Evaluation of natural pozzolan for use as supplementary cementitious material. *European Journal of Environmental and Civil Engineering*, 16(1), 77–96. doi:10.1080/19648189.2012.667692

Shannag, M. J., & Asim Yeginobali, A. (1995). Properties of pastes, mortars and concretes containing natural pozzolan. *Cement and Concrete Research*, *25*(3), 647–657. doi:10.1016/0008-8846(95)00053-F

Shi, C., & Day, R. (1993). Chemical activation of blended cements made with lime and natural pozzolans. *Cement and Concrete Research*, *23*, 1389–1396. doi:10.1016/0008-8846(93)90076-L

Turanli, L., Uzal, B., & Bektas, F. (2004). Effect of material characteristics on the properties of blended cements containing high volumes of natural pozzolans. *Cement & Concrete Research*, *34*, 2277–2282. doi:10.1016/j.cemconres.2004.04.011